

Fig. 7. Comparative analysis between DF and AF relaying protocols when the outage probability becomes saturated.

performance gap between DF and AF increases when the CD gets higher (i.e., when N increases).

REFERENCES

- [1] A. Sendonaris, E. Erkip, and B. Aazhang, "User cooperation diversity—Part I: System description," *IEEE Trans. Commun.*, vol. 51, no. 11, pp. 1927–1938, Nov. 2003.
- [2] J. N. Laneman, D. N. C. Tse, and G. W. Wornell, "Cooperative diversity in wireless networks: Efficient protocols and outage behavior," *IEEE Trans. Inf. Theory*, vol. 50, no. 12, pp. 3062–3080, Dec. 2004.
- [3] J. Mitola, III, "Cognitive radio: Making software radios more personal," *IEEE Pers. Commun.*, vol. 6, no. 4, pp. 13–18, Aug. 1999.
- [4] A. Ghasemi and E. S. Sousa, "Fundamental limits of spectrum-sharing in fading environments," *IEEE Trans. Wireless Commun.*, vol. 6, no. 2, pp. 649–658, Feb. 2007.
- [5] C. Zhong, T. Ratnarajah, and K.-K. Wong, "Outage analysis of decode-and-forward cognitive dual-hop systems with the interference constraint in Nakagami- m fading channels," *IEEE Trans. Veh. Technol.*, vol. 60, no. 6, pp. 2875–2879, Jul. 2011.
- [6] J. Lee, H. Wang, J. G. Andrews, and D. Hong, "Outage probability of cognitive relay networks with interference constraints," *IEEE Trans. Wireless Commun.*, vol. 10, no. 2, pp. 390–395, Feb. 2011.
- [7] T. Q. Duong, V. N. Q. Bao, G. C. Alexandropoulos, and H.-J. Zepernick, "Cooperative spectrum sharing networks with AF relay and selection diversity," *IET Electron. Lett.*, vol. 47, no. 20, pp. 1149–1151, Sep. 2011.
- [8] T. Q. Duong, D. B. da Costa, M. ElKashlan, and V. N. Q. Bao, "Cognitive amplify-and-forward relay networks over Nakagami- m fading," *IEEE Trans. Veh. Technol.*, vol. 61, no. 5, pp. 2368–2374, Jun. 2012.
- [9] T. Q. Duong, D. B. da Costa, T. A. Tsiftsis, C. Zhong, and A. Nallanathan, "Outage and diversity of cognitive relaying systems under spectrum sharing environments in Nakagami- m fading," *IEEE Commun. Lett.*, vol. 16, no. 12, pp. 2075–2078, Dec. 2012.
- [10] L. Luo, P. Zhang, G. Zhang, and J. Qin, "Outage performance for cognitive relay networks with underlay spectrum sharing," *IEEE Commun. Lett.*, vol. 15, no. 7, pp. 710–712, Jul. 2011.
- [11] A. Papoulis, *Probability, Random Variables, and Stochastic Processes*, 4th ed. New York, NY, USA: McGraw-Hill, 2002.
- [12] M. A. B. de Melo and D. B. da Costa, "An efficient relay-destination selection scheme for multiuser multirelay downlink cooperative networks," *IEEE Trans. Veh. Technol.*, vol. 61, no. 5, pp. 2354–2360, Jun. 2012.
- [13] D. B. da Costa and S. Aissa, "End-to-end performance of dual-hop semi-blind relaying systems with partial relay selection," *IEEE Trans. Wireless Commun.*, vol. 8, no. 8, pp. 4306–4315, Aug. 2009.
- [14] M. Abramowitz and I. A. Stegun, *Handbook of Mathematical Functions with Formulas, Graphs, and Mathematical Tables*. New York, NY, USA: U.S. Dept. Commerce, 1972.

Embedded Iterative Semi-Blind Channel Estimation for Three-Stage-Concatenated MIMO-Aided QAM Turbo Transceivers

Peichang Zhang, Sheng Chen, *Fellow, IEEE*, and Lajos Hanzo, *Fellow, IEEE*

Abstract—The lack of accurate and efficient channel estimation (CE) for multiple-input–multiple-output (MIMO) channel state information (CSI) has long been the stumbling block of near-MIMO-capacity operation. We propose a semi-blind joint CE and three-stage iterative detection/decoding scheme for near-capacity MIMO systems. The main novelty is that our decision-directed (DD) CE exploits the *a posteriori* information produced by the MIMO soft demapper within the inner turbo loop to select a "just sufficient number" of high-quality detected soft bit blocks or symbols for DDCE, which significantly improves the accuracy and efficiency of DDCE. Moreover, our DDCE is naturally embedded into the iterative three-stage detection/decoding process, without imposing an additional external iterative loop between the DDCE and the three-stage turbo detector/decoder. Hence, the computational complexity of our joint CE and three-stage turbo detector/decoder remains similar to that of the three-stage turbo detection/decoding scheme associated with the perfect CSI. Most significantly, the mean square error (MSE) of our DD channel estimator approaches the Cramér–Rao lower bound (CRLB) associated with the optimal-training-based CE, whereas the bit error rate (BER) of our semi-blind scheme is capable of achieving the optimal maximum-likelihood (ML) performance bound associated with the perfect CSI.

Index Terms—Cramér–Rao lower bound (CRLB), joint channel estimation and three-stage turbo detection/decoding, multiple-input–multiple-output (MIMO) systems, near-capacity.

I. INTRODUCTION

Under idealized conditions, coherent multiple-input–multiple-output (MIMO) systems are capable of achieving substantial diversity and/or multiplexing gains. However, the challenge is the acquisition of accurate MIMO channel state information (CSI) without imposing excessive pilot overhead, which would erode the system's throughput too much, and without resulting in potentially excessive channel estimation (CE) complexity. The current state of the art [1]–[16] typically combines the decision-directed (DD) CE (DDCE) with powerful iterative detection/decoding schemes to form semi-blind joint CE and turbo detection/decoding, where only a small number of training symbols are employed to generate an initial least squares channel estimate (LSCE). The turbo detection/decoding operation then commences with the initial LSCE. After the convergence of the turbo detector and decoder, the detected data are fed into the DDCE for the CE update. The DDCE and the turbo detector/decoder iterate a number of times until the channel estimate converges. The most effective schemes [10]–[13], [15], [16] employ soft-decision-aided channel estimators, which are more robust against error propagation than the hard-decision-aided CE schemes. Consequently, these joint soft-decision-based CE and turbo

Manuscript received November 16, 2012; revised March 4, 2013 and May 20, 2013; accepted June 25, 2013. Date of publication August 21, 2013; date of current version January 13, 2014. This work was supported in part by the Research Councils U.K. under the auspices of the India–U.K. Advanced Technology Center, by the European Union under the CONCERTO Project, and by the European Research Council under the Advanced Fellow Grant. The review of this paper was coordinated by Dr. T. Taniguchi.

The authors are with the School of Electronics and Computer Science, University of Southampton, Southampton SO17 1BJ, U.K. (e-mail: pz3g09@ecs.soton.ac.uk; sqc@ecs.soton.ac.uk; lh@ecs.soton.ac.uk).

Color versions of one or more of the figures in this paper are available online at <http://ieeexplore.ieee.org>.

Digital Object Identifier 10.1109/TVT.2013.2271872

detection/decoding schemes are capable of achieving better overall system performance than their hard-decision-based counterparts.

All these existing joint CE and turbo detection/decoding structures have a number of limitations. First, an extra iterative loop between the CE and the turbo detector/decoder is introduced, which considerably increases the complexity imposed. Second, existing schemes use the entire frame of the detected soft or hard bits for CE, and the complexity of the associated DD LSCE may become unacceptably high. This is because the number of bits in a single interleaved frame of a turbo code is very large, and typically, thousands of bits are contained in a turbo-coded frame. Third and most importantly, at low SNRs, practically 50% of the detected bits are erroneous; hence, the error propagation may be still serious even for soft-decision-aided CE schemes. Hence, error propagation would severely degrade the achievable performance. Therefore, all these existing schemes fail to approach the optimal maximum-likelihood (ML) turbo detection performance bound associated with the perfect CSI. In other words, even the best known joint CE and turbo detection/decoding schemes are incapable of attaining the optimal performance bound of the idealized ML turbo detector/decoder associated with the perfect CSI. Hence, it would appear that it is necessary to implant substantial pilot overhead, which dramatically erodes the system's throughput.

The objective of this paper is to demonstrate that the optimal MIMO performance may be nonetheless approached with the aid of very modest training overhead and without a significant increase in computational complexity. Specifically, we develop a novel joint CE and three-stage iterative detection/decoding structure¹ for near-capacity MIMO systems [19]. Our original contribution is twofold.

- 1) First, we propose a block-of-bits-selection-based soft-decision-aided CE (BBSB-SCE) scheme, which selects high-quality or more reliable detected symbols or blocks of bits based on the *a posteriori* information produced by the MIMO soft demapper within the original inner turbo loop of the unity-rate-code (URC) decoder and the MIMO detector advocated. Since our BBSB-SCE scheme only utilizes a "just sufficient number" of the high-quality detected symbols for CE, in contrast to the existing state-of-the-art solutions, it does not suffer from the usual performance degradation imposed by erroneous decisions. Furthermore, this measure dramatically reduces the complexity of the DD LSCE.
- 2) Second, our CE is naturally embedded in the original three-stage turbo detection/decoding process, and no extra iterative loop is required between the CE and the three-stage MIMO detector/decoder. Hence, the complexity of our joint BBSB-SCE and three-stage turbo detector/decoder remains similar to that of the idealized three-stage turbo receiver relying on the perfect CSI. We will show that our scheme is capable of attaining the optimal ML performance bound of the idealized three-stage turbo detector/decoder associated with the perfect CSI, despite using the same number of turbo iterations as the latter.

II. JOINT CE AND THREE-STAGE TURBO RECEIVER

We consider a MIMO system relying on N_T transmit antennas and N_R receive antennas for communication in a frequency-flat Rayleigh

fading environment. High-order quadrature amplitude modulation (QAM) [21] is used.

A. MIMO System Model

The transmitter consists of a two-stage serial-concatenated outer recursive systematic code (RSC) encoder combined with an inner URC encoder, followed by the MIMO-aided L -QAM modulator. This scheme is capable of achieving a near-capacity performance under idealized conditions [19]. The number of bits per L -QAM symbol (BPS) is given by $\text{BPS} = \log_2(L)$, and i denotes the symbol index. The MIMO system model is expressed as

$$\mathbf{y}(i) = \mathbf{H}\mathbf{s}(i) + \mathbf{v}(i) \quad (1)$$

where $\mathbf{H} \in \mathbb{C}^{N_R \times N_T}$ is the MIMO channel matrix whose elements obey the complex-valued zero-mean Gaussian distribution $\mathcal{CN}(0, 1)$ with a variance of $(1/2)$ per dimension, $\mathbf{s}(i) \in \mathbb{C}^{N_T}$ is the transmitted L -QAM symbol vector, $\mathbf{y}(i) \in \mathbb{C}^{N_R}$ is the received signal vector, and $\mathbf{v}(i) \in \mathbb{C}^{N_R}$ is the noise vector whose elements obey $\mathcal{CN}(0, N_o)$ with a variance of $(N_o/2)$ per dimension. The system's SNR is defined as $\text{SNR} = E_s/N_o$, where E_s is the average symbol energy.

Let us define the number of bits per block (BPB) as $\text{BPB} = N_T \cdot \text{BPS}$. At the receiver, upon obtaining the *a priori* log-likelihood ratios (LLRs) $\{L_a(u_k)\}_{k=1}^{\text{BPB}}$ from the channel decoder, where $\{u_k\}_{k=1}^{\text{BPB}}$ indicate the corresponding bits that are mapped to the symbol vector $\mathbf{s}(i)$, the *a posteriori* LLRs produced by the ML MIMO soft demapper² are expressed as [22]

$$L_p(u_k) = L_p(k) = \ln \frac{\sum_{\mathbf{s}^n \in \{\mathbf{s}_{u_k=1}\}} \exp(p_n)}{\sum_{\mathbf{s}^n \in \{\mathbf{s}_{u_k=0}\}} \exp(p_n)} \quad (2)$$

where $\{\mathbf{s}_{u_k=1}\}$ and $\{\mathbf{s}_{u_k=0}\}$ represent the L -QAM symbol-vector sets with the corresponding bits $u_k = 1$ and $u_k = 0$, respectively. The probability metrics $\{p_n\}_{n=1}^{L N_T}$ for the possible L -QAM symbol vectors $\{\mathbf{s}^n\}_{n=1}^{L N_T}$ are given as

$$p_n = -\frac{\|\mathbf{y}(i) - \mathbf{H}\mathbf{s}^n\|^2}{N_o} + \sum_{k=1}^{\text{BPB}} \tilde{u}_k L_a(u_k) \quad (3)$$

where $\{\tilde{u}_k\}_{k=1}^{\text{BPB}}$ indicate the corresponding bits that map to the specific symbol vector \mathbf{s}^n .

B. State of the Art

The state of the art [1]–[16] can be represented by the conventional joint CE and three-stage turbo detector/decoder structure³ shown in Fig. 1. For initiating the joint CE and three-stage turbo detection/decoding process, an initial training-based channel estimate is required. Let us assume that the number of available training blocks is M_T and the initial training data are arranged as $\mathbf{Y}_{tM_T} = [\mathbf{y}(1) \mathbf{y}(2) \cdots \mathbf{y}(M_T)]$ and $\mathbf{S}_{tM_T} = [\mathbf{s}(1) \mathbf{s}(2) \cdots \mathbf{s}(M_T)]$. Then, the LSCE of the MIMO channel matrix \mathbf{H} is given by

$$\hat{\mathbf{H}}_{\text{LSCE}} = \mathbf{Y}_{tM_T} \mathbf{S}_{tM_T}^H (\mathbf{S}_{tM_T} \mathbf{S}_{tM_T}^H)^{-1} \quad (4)$$

¹The low-complexity memory-1 URC adopted has an infinite impulse response, which allows the system to spread the extrinsic information beneficially across the iterative decoder components without increasing its delay. Therefore, the extrinsic information transfer (EXIT) curve is capable of reaching the (1.0, 1.0) point of perfect convergence in the EXIT charts, which is a necessary condition for near-capacity operation and for achieving a vanishingly low BER [17]–[20].

²For large MIMO systems, we may opt for using reduced-complexity near-optimal detection schemes, e.g., the K -best sphere detector [23], [24], to avoid the exponentially increasing complexity imposed by the ML detector.

³Most of these schemes were originally designed for the two-stage turbo detector/decoder structure, but they can be readily extended to the three-stage turbo detector/decoder structure discussed here.

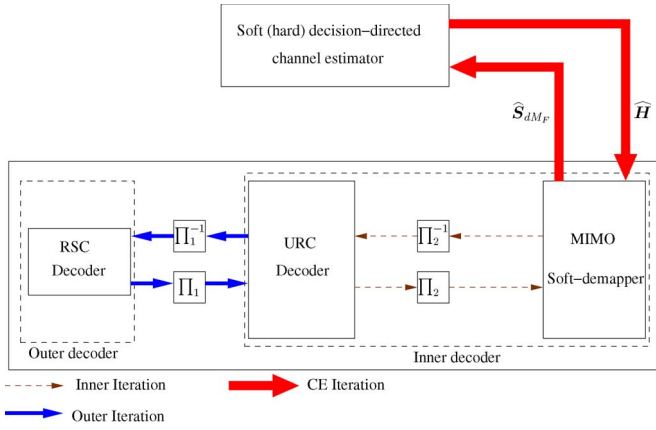


Fig. 1. Conventional joint CE and three-stage turbo detector/decoder, where $\hat{\mathbf{S}}_{dM_F}$ denotes all the soft- or hard-detected symbol blocks corresponding to the received data frame. Note that all the detected bits are used by the DD channel estimator. To benefit from the full error-correcting capability of the three-stage turbo detection/decoding, the updating of the DDCE takes place after the convergence of the outer turbo loop.

where $(\cdot)^H$ denotes the conjugate transpose operator. To maintain a high system throughput, only a small number of training blocks is used. To ensure a full rank for $\mathbf{S}_{tM_T} \mathbf{S}_{tM_T}^H$, it is necessary to choose $M_T \geq N_T$. Therefore, N_T is a lower bound for the number of initial training blocks. With M_T chosen to be close to its lower bound N_T , the accuracy of the LSCE (4) is poor; hence, the achievable bit error rate (BER) based on this initial LSCE is also poor. However, the three-stage turbo detector/decoder is capable of improving the reliability of the detected bits to assist the soft DDCE, which then provides a more accurate channel estimate. This iterative process results in an increasingly more reliable turbo detector/decoder output. It is observed in Fig. 1 that, since all the detected bits are used by the channel estimator, the DDCE update operation takes place after the convergence of the three-stage turbo detection/decoding, to fully exploit the error-correcting capability of the three-stage turbo detector/decoder. This introduces the additional CE loop shown in Fig. 1.

Let M_F be the length of the MIMO observation data sequence, which is arranged as

$$\mathbf{Y}_{dM_F} = [\mathbf{y}(1) \mathbf{y}(2) \cdots \mathbf{y}(M_F)]. \quad (5)$$

Let C_{RSC} , C_{URC} , and C_{ML} denote the computational complexity of the RSC decoder, the URC decoder, and the ML soft demapper, respectively. Assume that, given the CSI, the two-stage inner turbo loop requires I_{in} iterations, whereas the outer turbo loop requires I_{out} iterations. Then, given the CSI, the computational complexity of the three-stage turbo receiver can be formulated as

$$C_{\text{ideal}} = I_{\text{out}} (C_{\text{RSC}} + I_{\text{in}}(C_{\text{ML}} + C_{\text{URC}})). \quad (6)$$

The CE loop in Fig. 1 requires I_{ce} iterations to converge, and the computational complexity of its CE is on the order of M_F^3 or $\mathcal{O}(M_F^3)$, which is extremely high, considering that M_F is typically in the thousands. Thus, the overall computational complexity of the conventional joint CE and three-stage turbo receiver can be expressed as

$$C_{\text{con}} = I_{\text{ce}} \cdot \mathcal{O}(M_F^3) + I_{\text{ce}} \cdot C_{\text{ideal}} \quad (7)$$

which is significantly higher than C_{ideal} . More importantly, the frame of the detected bits may contain a large percentage of erroneous decisions, particularly at the low SNRs, which will degrade even the soft DD channel estimator that utilize all the soft-detected symbol blocks $\hat{\mathbf{S}}_{dM_F}$ corresponding to the received data frame \mathbf{Y}_{dM_F} . Therefore,

the existing conventional joint CE and three-stage turbo receivers fail to approach the optimal BER performance bound of the idealized three-stage turbo ML detector/decoder associated with the perfect CSI [10]–[12].

C. Joint BBSB-SCE and Three-Stage Turbo Receiver

The novel structure of our proposed BBSB-SCE and three-stage turbo detector/decoder is shown in Fig. 2. Note that there is no additional iterative loop involving the CE and the three-stage turbo detector/decoder. In other words, our soft-decision-aided CE is embedded in the original outer loop of the three-stage turbo structure, and the CE update concurrently occurs with the original outer turbo decoding iteration. Moreover, our CE does not use the entire frame of the detected bits. Rather, it only selects the high-quality or reliable decisions. Specifically, the *a posteriori* information (2) output by the MIMO soft demapper provides the confidence levels of binaries 1's and 0's [19]. Therefore, based on this confidence level, we can select the reliable decisions from the MIMO soft demapper's output sequence for CE. Removing most of the erroneous decisions from the CE leads to a much more accurate channel estimate, which in turn enhances the performance of the three-stage turbo detection/decoding process. Consequently, our joint BBSB-SCE and three-stage turbo detector/decoder is capable of attaining the performance bound of the idealized three-stage turbo ML-detector/decoder associated with the perfect CSI, as will be confirmed in our simulation study. As a further benefit of only selecting reliable decisions, the complexity of our soft-decision-aided LSCE is dramatically lower than $\mathcal{O}(M_F^3)$. Let us now detail our scheme further.

Step 1) Set the outer turbo iteration index to $t = 0$ and the initial channel estimate to $\hat{\mathbf{H}}^{(t)} = \hat{\mathbf{H}}_{\text{LSCE}}$.

Step 2) Given $\hat{\mathbf{H}}^{(t)}$, perform the ML soft demapping for the observation data \mathbf{Y}_{dM_F} of (5). The MIMO soft demapper exchanges its soft information with the URC inner decoder for I_{in} iterations, yielding the I_{in} vectors of the *a posteriori* information, as defined in (2), which can be arranged as the following *a posteriori* information matrix:

$$\mathbf{L}_p = [\mathbf{l}_p^1 \mathbf{l}_p^2 \cdots \mathbf{l}_p^{I_{\text{in}}}]^T \in \mathbb{C}^{I_{\text{in}} \times L_F} \quad (8)$$

where $(\cdot)^T$ denotes the transpose operator, $L_F = \text{BPB} \cdot M_F$ is the total number of bits in a frame, and $\mathbf{l}_p^i = [L_p^i(1) \ L_p^i(2) \ \cdots \ L_p^i(L_F)]^T \in \mathbb{C}^{L_F}$ for $1 \leq i \leq I_{\text{in}}$ is the *a posteriori* information vector obtained during the i th inner iteration. The n th column of \mathbf{L}_p contains the I_{in} soft decisions $\{L_p^1(n), L_p^2(n), \dots, L_p^{I_{\text{in}}}(n)\}$ for the n th information bit obtained in the I_{in} inner decoder iterations, which we exploit to judge whether the n th detected bit is reliable or not. Specifically, the n th detected bit is judged to be of high quality when either of the following two criteria is met.

Criterion 1: If the soft decisions in the n th column of \mathbf{L}_p share similar values, these soft decisions may result in a stable and reliable bit decision, which is hence considered correct. Specifically, the criterion for the n th detected bit to be judged as a correct one is

$$\frac{|L_p^1(n) - L_p^2(n)| + \cdots + |L_p^{I_{\text{in}}-1}(n) - L_p^{I_{\text{in}}}(n)|}{|\mu|} \in (0, T_h) \quad (9)$$

where μ is the mean of the soft decisions in the n th column of \mathbf{L}_p , and T_h denotes the predefined block-of-bits selection threshold.

Criterion 2: If the absolute values of the soft decisions in the n th column of \mathbf{L}_p are in monotonically ascending order and these soft decisions share the same sign, i.e.,

$$\left|L_p^1(n)\right| < \left|L_p^2(n)\right| < \cdots < \left|L_p^{I_{in}}(n)\right| \text{ and}$$

$$\text{sign}\{L_p^1(n)\} = \text{sign}\{L_p^2(n)\} = \cdots = \text{sign}\{L_p^{I_{in}}(n)\}$$

the n th detected bit may be regarded as a correct one.

By checking through the columns of \mathbf{L}_p , only high-confidence decision blocks are selected, and the corresponding symbol block indices can be determined by a sliding-window method using a window size of BPB bits. More explicitly, only when the BPB consecutive detected bits of a block are all regarded as correct that the corresponding symbol vector is selected for CE. This process yields an integer-index vector, denoted as $\mathbf{x}^t = [x^t(1) \ x^t(2) \ \cdots \ x^t(M_s^t)]^T$, in which $x^t(i)$ is the position or index of the i th selected symbol vector in the transmitted symbol-vector sequence. The number of the selected symbol vectors M_s^t varies within $\{1, 2, \dots, M_{\text{sel}}\}$, where $M_{\text{sel}} \ll M_F$ is the maximum number of blocks imposed for CE. Specifically, whenever the number of selected reliable symbol vectors M_s^t reaches the limit M_{sel} , the sliding-window process ends; otherwise, the sliding-window process examines all the possible bit blocks and outputs the M_s^t selected symbol vectors. Thus, M_s^t varies at each outer turbo iteration t , and $M_s^t \leq M_{\text{sel}}$. By using this index vector, the corresponding observation data can be selected from (5) and rearranged as

$$\mathbf{Y}_{\text{sel}}^{(t)} = [\mathbf{y}(x^t(1)) \ \mathbf{y}(x^t(2)) \ \cdots \ \mathbf{y}(x^t(M_s^t))]. \quad (10)$$

Step 3) Based on the selected high-confidence detected blocks of bits having the symbol-vector indices \mathbf{x}^t , generate the soft-estimate of each symbol element as [13]

$$\begin{aligned} \hat{s}^m(x^t(n)) &= \sum_{l=1}^L s^l \Pr\{s^m(x^t(n)) = s^l\} \\ &= \sum_{l=1}^L s^l \cdot \frac{\exp\left(\sum_{j=1}^{\text{BPS}} \tilde{u}_j L_a(u_j)\right)}{\prod_{j=1}^{\text{BPS}} (1 + \exp L_a(u_j))} \end{aligned} \quad (11)$$

for $1 \leq n \leq M_s^t$, where $\{s^l\}_{l=1}^L$ denotes the L -QAM symbol set, $m \in \{1, 2, \dots, N_T\}$ indicates the symbol index in the soft-estimated symbol vector $\hat{\mathbf{s}}(x^t(n))$, and $\{\tilde{u}_j\}_{j=1}^{\text{BPS}}$ represents the bit mapping corresponding to $\{s^l\}_{l=1}^L$. By arranging the soft-estimated symbol vectors as

$$\hat{\mathbf{S}}_{\text{sel}}^{(t)} = [\hat{\mathbf{s}}(x^t(1)) \ \hat{\mathbf{s}}(x^t(2)) \ \cdots \ \hat{\mathbf{s}}(x^t(M_s^t))] \quad (12)$$

and by defining $\mathbf{Y}_{t+\text{sel}}^{(t)} = [\mathbf{Y}_{tM_T} \ \mathbf{Y}_{\text{sel}}^{(t)}]$ and $\hat{\mathbf{S}}_{t+\text{sel}}^{(t)} = [\mathbf{S}_{tM_T} \ \hat{\mathbf{S}}_{\text{sel}}^{(t)}]$, the resulting DD LSCE is given by

$$\hat{\mathbf{H}}^{(t+1)} = \mathbf{Y}_{t+\text{sel}}^{(t)} \left(\hat{\mathbf{S}}_{t+\text{sel}}^{(t)}\right)^H \left(\hat{\mathbf{S}}_{t+\text{sel}}^{(t)} \left(\hat{\mathbf{S}}_{t+\text{sel}}^{(t)}\right)^H\right)^{-1}. \quad (13)$$

This update occurs as the soft information is exchanged between the two-stage inner decoder and the outer RSC decoder, as indicated in Fig. 2.

Step 4) Set $t = t + 1$. If $t < I_{\text{out}}$, repeat Steps 2 and 3; otherwise, stop.

The computational complexity of our CE is upper bounded by $\mathcal{O}(M_{\text{sel}}^3)$, which is much smaller than $\mathcal{O}(M_F^3)$. For example, considering a reasonable case of $M_F = 1000$ and $M_{\text{sel}} = 100$, the complexity

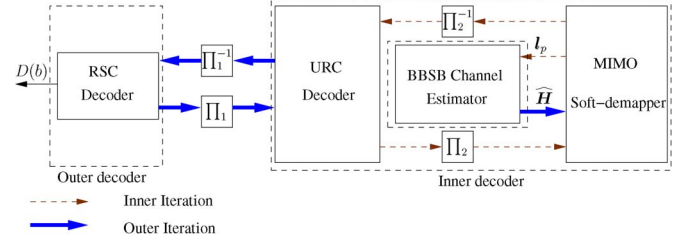


Fig. 2. Proposed joint BBSB-SCE and three-stage turbo detector/decoder. Because only reliable detected bit blocks are utilized in the DDCE, there is no need to wait for the convergence of the three-stage turbo detector/decoder, and the updating of the DDCE can concurrently take place with the outer turbo iteration.

of our CE is more than 1000 times smaller than that of the conventional scheme. The total complexity of our proposed scheme satisfies

$$C_{\text{pro}} \leq I_{\text{out}} \cdot \mathcal{O}(M_{\text{sel}}^3) + C_{\text{ideal}}. \quad (14)$$

Since $I_{\text{out}} \cdot \mathcal{O}(M_{\text{sel}}^3) \ll C_{\text{ideal}}$, we have $C_{\text{pro}} \approx C_{\text{ideal}}$.

Remark 1: We now elaborate on the two criteria used for selecting high-quality bits. The idea behind *Criterion 1* is that, if the decisions for the n th bit are relatively similar during the inner turbo iterations, the n th bit decision may be regarded as reliable. This makes sense because, following a number of outer iterations, a stable state may be reached by the turbo decoder; hence, the stable decisions of the inner decoder are likely to be the correct decisions. Our experience suggests that most of the chosen bit blocks or symbols are selected according to *Criterion 1*.

As for *Criterion 2*, we note that, if the absolute values of the decisions for a specific bit are in monotonically ascending order and these decisions share the same polarity, the corresponding bit decision is likely to be correct. This makes sense because the correct decisions may experience iteration gain, and this will lead to increasing absolute values of the soft decisions as the number of inner iterations increases. This type of reliable decisions could be missed according to *Criterion 1*; hence, *Criterion 2* allows us to select these high-quality decisions when they do occur.

An important point to note is that our scheme fully exploits the information provided by the entire inner turbo iterative process, as manifested in the n th column of the *a posteriori* information matrix \mathbf{L}_p in (8). Therefore, it is capable of making a high-confidence decision regarding whether the n th detected bit is reliable or not.

Remark 2: For binary phase-shift keying (BPSK) signaling, the work of Abe and Matsumoto [25] also selects reliable decisions for DDCE. Specifically, a soft symbol estimate is directly obtained from the bit's LLR [25], owing to the one bit per symbol nature of BPSK. The magnitude of the soft symbol estimate provides an estimated probability of the symbol, which is then used to decide whether the particular bit or symbol decision is reliable or not. However, it is impossible to extend the decision selection algorithm of [25] to the generic high-order QAM-aided system. To the best of our knowledge, our method is the only available algorithm that can be used to select high-quality decisions for the generic QAM case. Moreover, even for BPSK signaling, the symbol probability estimate given in [25] itself may not always be reliable. This is indeed confirmed by the original simulation results for the BPSK case presented in [25], where it is shown that the performance loss is large at low SNRs in comparison with the perfect CSI performance bound. Indeed, the estimated probability of the n th bit or symbol is based on the single LLR $L_p^{I_{in}}(n)$ [25]. By contrast, our scheme utilizes all the I_{in} LLRs provided by the inner iterative process to decide whether the n th detected bit or symbol is correct. We have also compared our algorithm with the decision selection algorithm in

[25] designed for near-capacity BPSK MIMO systems, and the results obtained confirm that our scheme outperforms the scheme in [25].

Remark 3: The value of the block-of-bits selection threshold T_h employed in Step 2 for *Criterion 1* should be carefully chosen. A very small value may lead to an insufficient number of blocks selected for CE even after examining the entire sequence of L_F bit decisions. By contrast, a very large value may result in the number of selected blocks reaching the limit value M_{sel} after only examining a small initial portion of the L_F bit decisions, and the selected blocks may contain many “low confidence” decisions. Both of these two situations will result in performance degradation. However, apart from these relatively extreme cases, our experience suggests that the performance of our semi-blind scheme is insensitive to the value of T_h . Specifically, there exists a relatively wide range of values for T_h , which allows our scheme to approach its optimal performance without increasing the number of turbo iterations. This range of optimal values for T_h depends on both the modulation scheme and on the MIMO channel.

III. SIMULATION RESULTS AND DISCUSSIONS

Example 1: A quasi-static Rayleigh fading MIMO system using $N_T = N_R = 4$ and 16-QAM was simulated. An interleaver length of $L_F = 16000$ bits was used, yielding $M_F = 1000$ for each 16-QAM symbol-vector frame. The binary generator polynomials of the half-rate RSC encoder were $G_{RSC} = [1, 0, 1]_2$ and $G_{RSC}^r = [1, 1, 1]_2$, whereas those of the URC encoder were $G_{URC} = [1, 0]_2$ and $G_{URC}^r = [1, 1]_2$. The transmitted signal power was normalized to unity; therefore, the SNR was given as $(1/N_o)$. The number of initial training data blocks was chosen to be $M_T = 6$, yielding a training overhead of 0.6%, whereas the maximum number of selected blocks for our BBSB-SCE was limited to $M_{sel} = 100$. At the beginning of each frame, a new MIMO channel matrix \mathbf{H} was generated by randomly drawing the channel taps according to $\mathcal{CN}(0, 1)$, and \mathbf{H} was kept constant in the frame duration. Two metrics were used to assess the achievable performance, namely, the BER and the MSE of the CE. The Cramér–Rao lower bound (CRLB) [26] is known to provide the best attainable performance for an unbiased estimator and can be used for lower bounding the MSE of a CE.

The BER performance of the proposed joint BBSB-SCE and three-stage turbo receiver is shown in Fig. 3, in comparison with that of the perfect CSI bound and those of the conventional semi-blind joint CE and three-stage turbo schemes utilizing the entire detected data sequence for the soft- and hard-decision-aided CEs, respectively. Our semi-blind joint BBSB-SCE and three-stage turbo detector/decoder employed $I_{in} = 3$ inner turbo iterations and $I_{out} = 5$ outer turbo iterations, which were identical to those employed by the idealized three-stage turbo detector/decoder associated with the perfect CSI. It can be seen that the proposed semi-blind BBSB-SCE scheme is capable of attaining the near-capacity optimal ML performance associated with the perfect CSI, with the same “turbo-cliff” occurring before SNR = 5 dB. The conventional joint CE and three-stage turbo receiver combined with the soft-decision-aided CE employing the entire detected data sequence cannot attain the perfect CSI performance bound, and there is a 2-dB gap between the BER turbo-cliffs of the two receivers. The conventional scheme employing the hard-decision-aided CE based on the entire detected data sequence exhibits further degradation of 1.5 dB from its soft-decision-assisted counterpart.

Fig. 4 shows the convergence behavior of the proposed joint BBSB-SCE and three-stage turbo scheme. It can be seen that the BER gap between the proposed BBSB-SCE-based scheme and the perfect CSI case reduces as the number of outer iterations increases. Specifically, after the initial iteration, there is a large BER gap, whereas during the third iteration, the BER gap is reduced to around 1 dB. Finally, at the

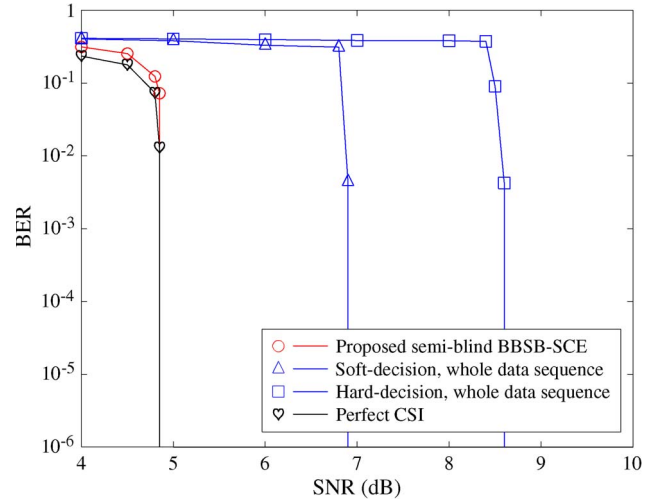


Fig. 3. BER performance comparison. (a) Perfect CSI case. (b) Proposed joint BBSB-SCE and three-stage turbo receiver with $T_h = 1.0$. (c) Conventional joint CE and three-stage turbo receivers employing the entire detected data sequence for the soft- and hard-decision-aided channel estimators, respectively, for *Example 1* of the quasi-static MIMO system.

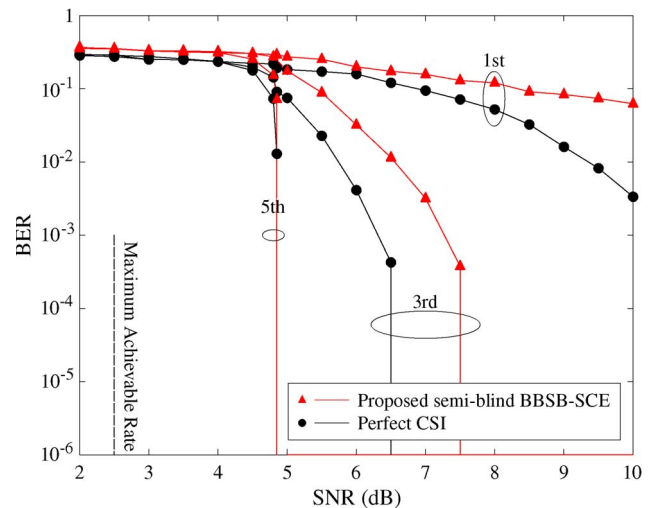


Fig. 4. Convergence performance of the proposed joint BBSB-SCE and three-stage turbo detector/decoder with $T_h = 1$, in comparison with the perfect-CSI case for *Example 1* of the quasi-static MIMO system.

fifth iteration, there is no BER gap, indicating that the BBSB-SCE scheme has converged to the true MIMO carrier-to-interference ratio. This is very significant since our semi-blind BBSB-SCE-based scheme has training overhead as low as 0.6%; however, it attains the optimal performance of the idealized three-stage turbo receiver associated with perfect CSI while only imposing complexity similar to the latter, as evidenced by our complexity comparison given in (14). The effects of the selection threshold T_h on the achievable performance of our proposed semi-blind scheme were investigated by varying the value of T_h in the set $\{0.2, 0.5, 1.0, 2.0, 3.0\}$. The results obtained are shown in Fig. 5, where it is shown that $T_h \in [0.5, 1.0]$ in this example allows our scheme to approach the perfect CSI performance bound. The MSE performance of the CE in our proposed scheme is compared with the CRLB associated with the optimal training sequence of length $M_T^{opt} = 100$ in Fig. 6, where it can be seen that the MSE of our DDCE approaches the CRLB once the number of outer turbo iterations reaches $I_{out} = 5$ for $\text{SNR} \geq 5$ dB. This corresponds to the BER cliff at SNR of ≈ 5 dB and $I_{out} = 5$ shown in Fig. 3.

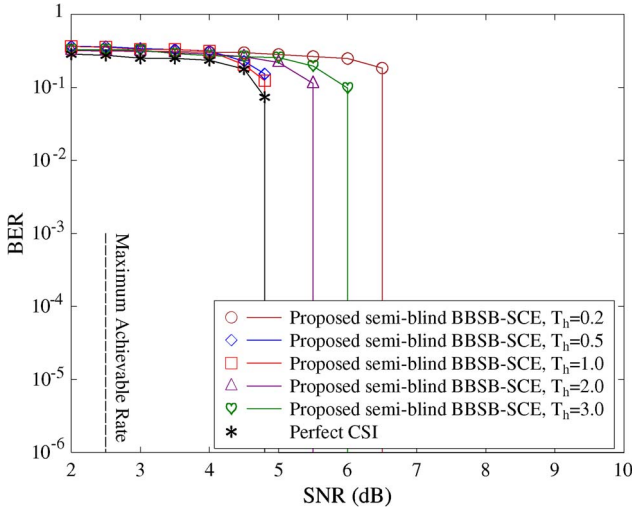


Fig. 5. Effects of the block-of-bits selection threshold T_h on the achievable BER performance for *Example 1* of the quasi-static MIMO system.

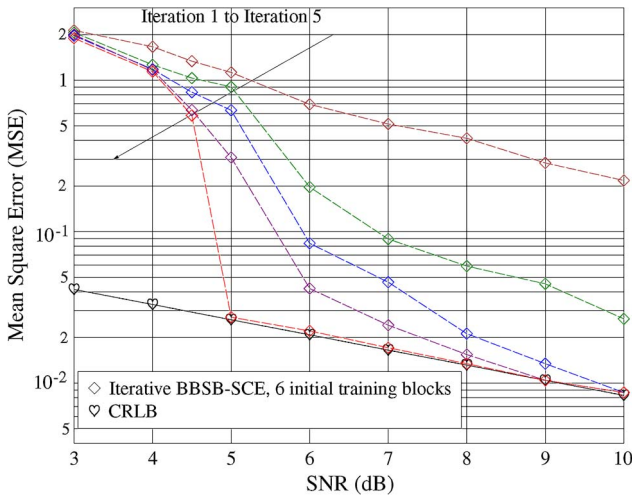


Fig. 6. MSE convergence performance of the CE in our proposed semi-blind joint BBSB-SCE and three-stage turbo detection/decoding scheme using a block-of-bits selection threshold of $T_h = 1.0$ for *Example 1* of the quasi-static MIMO system.

Example 2: The system setup was identical to that of *Example 1*, except that the MIMO channels were time-varying. Specifically, \mathbf{H} was faded at the symbol rate during each frame according to the normalized Doppler frequency of f_d . Note that, for the time-varying MIMO system, there exists a tradeoff between the time-varying channel’s estimation (TVCE) performance and the turbo channel decoder’s performance. To be more explicit, for turbo channel coding, a long interleaver length L_F is preferred to achieve near-capacity performance [19]. However, a short frame length M_F , i.e., a short interleaver length L_F , is preferred to achieve a good TVCE performance. In our simulations, we varied f_d and investigated different interleaver lengths.⁴

Fig. 7 shows the results obtained for the case of the normalized Doppler frequency $f_d = 10^{-5}$ with $L_F = 16\,000, 8\,000$, and $4\,000$ bits, respectively, where it can be seen that, for each given interleaver length L_F , the proposed semi-blind joint BBSB-SCE relying on three-stage turbo receiver outperforms the conventional semi-blind

⁴In practice, the Doppler spread may be estimated using the schemes proposed in [27]–[29].

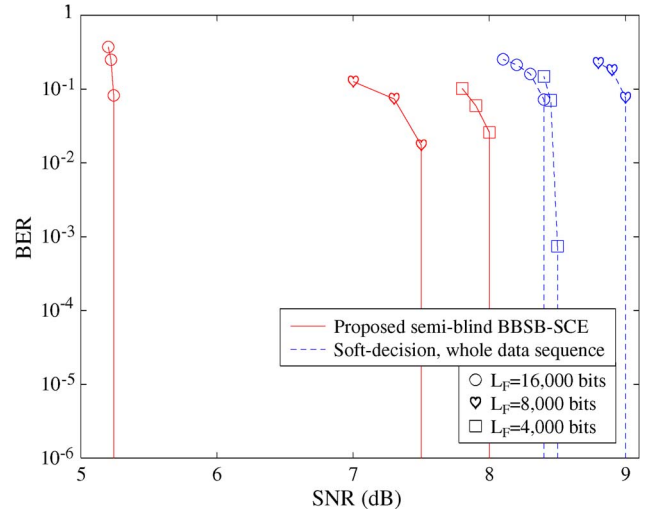


Fig. 7. BER performance comparison. (a) Proposed joint BBSB-SCE and three-stage turbo receiver with $T_h = 1$. (b) Conventional joint CE and three-stage turbo receiver employing the entire detected data sequence for the soft-decision-aided channel estimator for *Example 2* of the time-varying MIMO system with the normalized Doppler frequency $f_d = 10^{-5}$ and the interleaver lengths of $L_F = 16\,000, 8\,000$, and $4\,000$ bits, respectively.

joint CE and three-stage turbo scheme utilizing the entire detected data sequence. Specifically, our scheme achieves SNR gains of 3.1, 1.5, and 0.5 dB over the conventional one for $L_F = 16\,000$ bits, $L_F = 8\,000$ bits, and $L_F = 4\,000$ bits, respectively. As expected, our proposed semi-blind BBSB-SCE scheme achieves its best BER performance for the long interleaver length of $L_F = 16\,000$ bits. This is because the normalized Doppler frequency of $f_d = 10^{-5}$ represents a relatively slowly fluctuating channel. Hence, the achievable system performance is dominated by the performance of the iterative channel decoder that favors a high L_F value. Furthermore, as the interleaver length of our scheme reduces, the number of potential high-quality candidates may also be reduced, which may hence contribute to the degradation of the system’s performance.

A similar conclusion may be drawn for the conventional semi-blind CE scheme in Fig. 7, where the performance of the conventional scheme is degraded by about 0.6 dB, when the interleaver length is reduced from 16 000 to 8 000 bits. However, unlike for our proposed semi-blind BBSB-SCE scheme, in this particular case, the performance of the conventional semi-blind CE scheme recorded for $L_F = 4\,000$ bits is slightly better than that of the $L_F = 8\,000$ -bit scenario.

Fig. 8 compares the achievable BER performance of our proposed scheme to that of the conventional scheme for the case of the normalized Doppler frequency $f_d = 10^{-4}$ with $L_F = 16\,000, 8\,000$, and $4\,000$ bits, respectively. As shown in Fig. 8, the best performance is achieved with the interleaver length of $L_F = 4\,000$ bits, whereas the worst performance is obtained for the interleaver length of $L_F = 16\,000$ bits for both our proposed scheme and the conventional scheme. At the normalized Doppler frequency of $f_d = 10^{-4}$, the MIMO system’s overall performance is dominated by the TVCE performance, which favors a short interleaver. Evidently, there exists a tradeoff between the turbo channel coding performance and the TVCE performance in choosing the best interleaver length. It is furthermore observed in Fig. 8 that, for a given interleaver length L_F , our proposed scheme always outperforms the conventional scheme.

When considering an even higher normalized Doppler frequency of $f_d = 5 \times 10^{-4}$, both our proposed semi-blind joint BBSB-SCE relying on the three-stage turbo receiver and the conventional semi-blind joint CE and three-stage turbo scheme utilizing the entire detected data sequence for the soft-decision-aided CE cannot converge

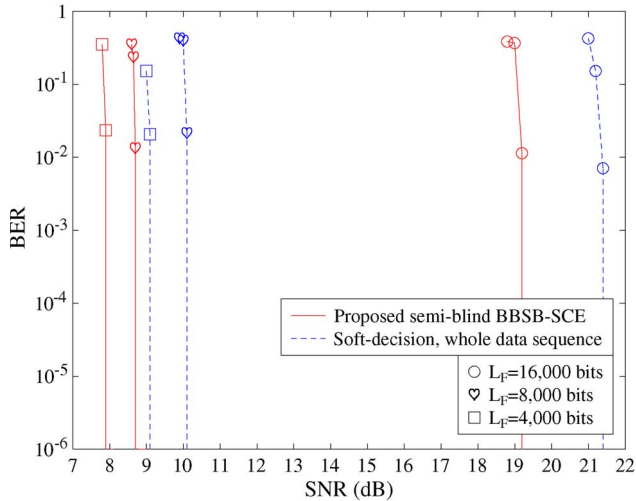


Fig. 8. BER performance comparison. (a) Proposed joint BBSB-SCE and three-stage turbo receiver with $T_h = 1$. (b) Conventional joint CE and three-stage turbo receiver employing the entire detected data sequence for the soft-decision-aided channel estimator for *Example 2* of the time-varying MIMO system with the normalized Doppler frequency $f_d = 10^{-4}$ and the interleaver lengths of $L_F = 16\,000$, $8\,000$, and $4\,000$ bits, respectively.

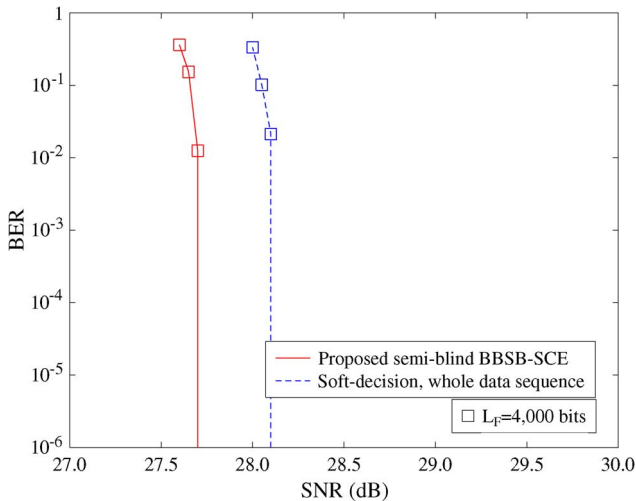


Fig. 9. BER performance comparison: (a) Proposed joint BBSB-SCE and three-stage turbo receiver with $T_h = 1$. (b) Conventional joint CE and three-stage turbo receiver employing the entire detected data sequence for the soft-decision-aided channel estimator for *Example 2* of the time-varying MIMO system with the normalized Doppler frequency $f_d = 5 \times 10^{-4}$ and the interleaver length of $L_F = 4\,000$ bits.

(there exists no open tunnel between the EXIT curves of the inner and outer decoders) for the interleaver lengths of $L_F = 16\,000$ bits and $L_F = 8\,000$ bits associated with an SNR as high as 30 dB. Evidently, using $L_F = 16\,000$ bits or $L_F = 8\,000$ bits is excessively long, which degrades the TVCE performance to an unacceptable level. However, when the interleaver length was reduced to $L_F = 4\,000$, both schemes become capable of achieving convergence, as shown in Fig. 9. It is observed in Fig. 9 that the proposed semi-blind BBSB-SCE scheme outperforms the conventional semi-blind CE scheme by about 0.4 dB.

Example 3: We also considered a quasi-static Rayleigh fading BPSK MIMO system associated with $N_T = N_R = 2$ and set the initial training block length to $M_T = 6$. The other system settings were the same as in *Example 1*. The simulation results shown in Fig. 10 compare our proposed BBSB-SCE scheme to the decision selection

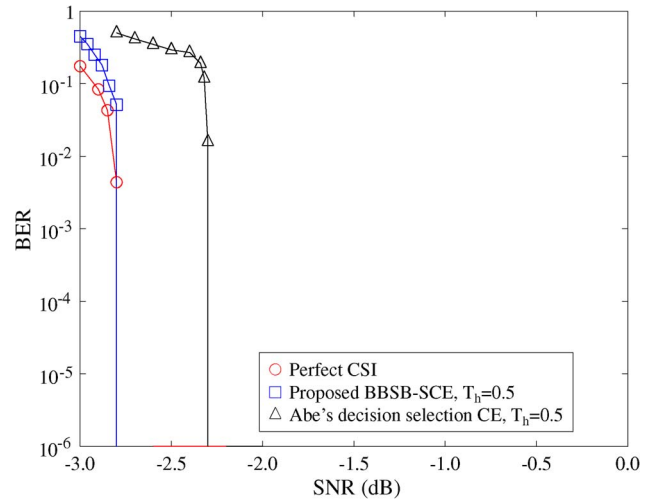


Fig. 10. BER performance comparison. (a) Perfect CSI case. (b) Proposed joint BBSB-SCE and three-stage turbo receiver with $T_h = 0.5$. (c) Abe and Matsumoto's BPSK-decision-selection-scheme-based soft CE [25] for *Example 3* of the quasi-static BPSK MIMO system with $N_T = N_R = 2$.

scheme of Abe and Matsumoto based on soft CE [25], using again the perfect CSI performance bound as the benchmark. It is explicitly shown in Fig. 10 that, as expected, our BBSB-SCE scheme approaches the optimal performance bound associated with the perfect CSI, and it slightly outperforms the scheme proposed by Abe and Matsumoto by about 0.5 dB.

IV. CONCLUSION

We have proposed a novel semi-blind joint BBSB-SCE and three-stage turbo detection/decoding scheme for near-capacity MIMO systems. Unlike all the existing methods, our scheme does not require an extra iterative loop between the channel estimator and the turbo detector/decoder since our BBSB-SCE is naturally embedded into the original three-stage demapping/decoding turbo loop. This novel arrangement enables us to substantially reduce the computational complexity. Most significantly, our BBSB-SCE scheme only selects high-confidence decisions for our soft-DDCE. This not only ensures that the complexity of our channel estimator is several orders of magnitude lower than that of the existing methods but also enables our scheme to attain the optimal ML performance of the idealized three-stage turbo receiver furnished with perfect CSI, using the same number of turbo iterations as the latter.

REFERENCES

- [1] M. Loncar, R. Muller, J. Wehinger, and T. Abe, "Iterative joint detection, decoding, and CE for dual antenna arrays in frequency selective fading," in *Proc. 5th Int. Symp. Wireless Pers. Multimedia Commun.*, Honolulu, HI, USA, Oct. 27–30, 2002, pp. 125–129.
- [2] M. Loncar, R. Muller, J. Wehinger, C. F. Mecklenbrauker, and T. Abe, "Iterative channel estimation and data detection in frequency-selective fading MIMO channels," *Eur. Trans. Telecommun.*, vol. 15, no. 5, pp. 459–470, Sep./Oct. 2004.
- [3] H. Li, S. M. Betz, and H. V. Poor, "Performance analysis of iterative channel estimation and multiuser detection in multipath DS-SS-CDMA channels," *IEEE Trans. Signal Process.*, vol. 55, no. 5, pp. 1981–1993, May 2007.
- [4] M. Jiang, J. Akhtman, and L. Hanzo, "Iterative joint CE and multi-user detection for multiple-antenna aided OFDM systems," *IEEE Trans. Wireless Commun.*, vol. 6, no. 8, pp. 2904–2914, Aug. 2007.
- [5] M. Qaisrani and S. Lambotharan, "An iterative (turbo) CE and symbol detection technique for doubly selective channels," in *Proc. VTC*, Dublin, Ireland, Apr. 22–25, 2007, pp. 2253–2256.

- [6] P. S. Rossi and R. R. Müller, "Joint twofold-iterative channel estimation and multiuser detection for MIMO-OFDM systems," *IEEE Trans. Wireless Commun.*, vol. 7, no. 11, pp. 4719–4729, Nov. 2008.
- [7] J. Ylioinas and M. Juntti, "Iterative joint detection, decoding, and channel estimation in turbo-coded MIMO-OFDM," *IEEE Trans. Veh. Technol.*, vol. 58, no. 4, pp. 1784–1796, May 2009.
- [8] J. Zhang, S. Chen, X. Mu, and L. Hanzo, "Joint CE and multi-user detection for SDMA/OFDM based on dual repeated weighted boosting search," *IEEE Trans. Veh. Technol.*, vol. 60, no. 7, pp. 3265–3275, Sep. 2011.
- [9] J. Zhang, S. Chen, X. Mu, and L. Hanzo, "Turbo multi-user detection for OFDM/SDMA systems relying on differential evolution aided iterative channel estimation," *IEEE Trans. Commun.*, vol. 60, no. 6, pp. 1621–1633, Jun. 2012.
- [10] M. Sandell, C. Luschi, P. Strauch, and R. Yan, "Iterative CE using soft decision feedback," in *Proc. GLOBECOM*, Sydney, Australia, Nov. 8–12, 1998, pp. 3728–3733.
- [11] S. Song, A. C. Singer, and K. Sung, "Soft input CE for turbo equalization," *IEEE Trans. Signal Process.*, vol. 52, no. 10, pp. 2885–2894, Oct. 2004.
- [12] B. Hu, A. Kocian, R. Piton, A. Hviid, B. H. Fleury, and L. K. Rasmussen, "Iterative joint CE and successive interference cancellation using a SISO-SAGE algorithm for coded CDMA," in *Proc. 38th Asilomar Conf. Signals, Syst. Comput.*, Pacific Grove, CA, USA, Nov. 7–10, 2004, pp. 622–626.
- [13] M. Sellathurai and S. Haykin, "Turbo-BLAST for wireless communications: Theory and experiments," *IEEE Trans. Signal Process.*, vol. 50, no. 10, pp. 2538–2546, Oct. 2002.
- [14] M. Nicoli, S. Ferrar, and U. Spagnolini, "Soft-iterative channel estimation: Methods and performance analysis," *IEEE Trans. Signal Process.*, vol. 55, no. 6, pp. 2993–3006, Jun. 2007.
- [15] Y. Wu, X. Zhu, and A. K. Nandi, "Soft-input turbo CE for single-carrier multiple-input-multiple-output systems," *IEEE Trans. Veh. Technol.*, vol. 58, no. 7, pp. 3867–3873, Sep. 2009.
- [16] W. Haselmayr, D. Schellander, and A. Springer, "Iterative CE and turbo equalization for time-varying channels in a coded OFDM-LTE system for 16-QAM and 64-QAM," in *Proc. 21st IEEE Int. Symp. Pers. Indoor Mobile Radio Commun.*, Istanbul, Turkey, Sep. 26–30, 2010, pp. 614–618.
- [17] I. Land, P. A. Hoeher, and S. Gligorevi, "Computation of symbol-wise mutual information in transmission systems with logAPP decoders and application to EXIT charts," in *Proc. 5th Int. ITG Conf. SCC*, Erlangen, Germany, Jan. 2004, pp. 195–202.
- [18] J. Wang, S. X. Ng, A. Wolfgang, L. L. Yang, S. Chen, and L. Hanzo, "Near-capacity three-stage MMSE turbo equalization using irregular convolutional codes," in *Proc. Turbo-Coding*, Munich, Germany, Apr. 3–7, 2006, pp. 1–6.
- [19] L. Hanzo, O. R. Alamri, M. El-Hajjar, and N. Wu, *Near-Capacity Multi-Functional MIMO Systems: Sphere-Packing, Iterative Detection and Cooperation*. Chichester, U.K.: Wiley, 2009.
- [20] R. G. Maunder and L. Hanzo, "Iterative decoding convergence and termination of serially concatenated codes," *IEEE Trans. Veh. Technol.*, vol. 90, no. 1, pp. 216–224, Jan. 2010.
- [21] L. Hanzo, S. X. Ng, T. Keller, and W. Webb, *Quadrature Amplitude Modulation: From Basics to Adaptive Trellis-Coded, Turbo-Equalised and Space-Time Coded OFDM, CDMA and MC-CDMA Systems*, 2nd ed. Chichester, U.K.: Wiley, 2004.
- [22] C. Xu, S. Sugiura, S. X. Ng, and L. Hanzo, "Spatial modulation and space-time shift keying: Optimal performance at a reduced detection complexity," *IEEE Trans. Commun.*, vol. 61, no. 1, pp. 206–216, Jan. 2013.
- [23] Z. Guo and P. Nilsson, "Algorithm and implementation of the K-best sphere decoding for MIMO detection," *IEEE J. Sel. Areas Commun.*, vol. 24, no. 3, pp. 491–503, Mar. 2006.
- [24] L. Wang, L. Xu, S. Chen, and L. Hanzo, "Apriori-LLR-threshold-assisted K-best sphere detection for MIMO channels," in *Proc. VTC*, Singapore, May 11–14, 2008, pp. 867–871.
- [25] T. Abe and T. Matsumoto, "Space-time turbo equalization in frequency-selective MIMO channels," *IEEE Trans. Veh. Technol.*, vol. 52, no. 3, pp. 469–475, May 2003.
- [26] S. M. Kay, *Fundamentals of Statistical Signal Processing: Estimation Theory*. Englewood Cliffs, NJ, USA: Prentice-Hall, 1993.
- [27] J. Hua, L. Meng, X. Xu, D. Wang, and X. You, "Novel scheme for joint estimation of SNR, Doppler, and carrier frequency offset in double-selective wireless channels," *IEEE Trans. Veh. Technol.*, vol. 58, no. 3, pp. 1204–1217, Mar. 2009.
- [28] J. Hua, L. Meng, G. Li, D. Wang, B. Sheng, and X. You, "Joint estimation of channel parameters for very low signal-to-noise ratio environment in mobile radio propagations," *Radio Sci.*, vol. 45, no. 4, pp. 1–8, Aug. 2010.
- [29] A. Dogandzic and B. Zhang, "Estimating Jakes' Doppler power spectrum parameters using the whittle approximation," *IEEE Trans. Signal Process.*, vol. 53, no. 3, pp. 987–1005, Mar. 2005.

QRD-Assisted Adaptive Modulation-Aided MIMO Systems

Ping Yang, Yue Xiao, Shaoqian Li, and Lajos Hanzo

Abstract—In this paper, we propose *QR*-decomposition (QRD)-based adaptive modulation (AM)-aided multiple-input-multiple-output (MIMO) systems. The proposed algorithm yields a tight lower bound of the free distance (FD), which determines the error probability of the detector in the high-signal-to-noise-ratio (SNR) region. Thus, this QRD-based AM algorithm is capable of achieving near-optimal performance at low complexity because the full QRD, which imposes high complexity, is performed only once for each channel realization, regardless of the number of AM modes. Our simulation results show that the proposed algorithm exhibits a better bit-error-rate (BER) performance and reduced complexity compared with the existing algorithms.

Index Terms—Adaptive modulation (AM), free distance (FD), multiple-input multiple-output (MIMO), *QR* decomposition (QRD).

I. INTRODUCTION

Multiple-input-multiple-output (MIMO) systems are capable of achieving a capacity gain and/or increased link robustness [1]–[3]. Hence, they have been adopted in most of the recent communication standards such as IEEE 802.11n, IEEE 802.16e, and Third-Generation Partnership Project Long-Term Evolution [4]. They may be also beneficially combined with adaptive modulation (AM) for adjusting the transmission parameters for the sake of accommodating time-varying channels [5]. Therefore, the effective combination of AM and MIMO techniques is a promising design alternative for high-rate wireless transmission systems [5], [6].

In MIMO systems, several AM-based link adaptation schemes [5]–[10] have been proposed for improving the achievable system performance. For example, the performance of AM-aided MIMO systems has been analyzed under both continuous- and discrete-rate scenarios in [7]. Moreover, adaptive MIMO architectures utilizing different combinations of modulation/coding schemes have been proposed in

Manuscript received January 6, 2013; revised May 20, 2013 and July 3, 2013; accepted July 20, 2013. Date of publication July 23, 2013; date of current version January 13, 2014. This work was supported in part by the Doctor Foundation of the Ministry of Education under Grant 20110185130003 and in part by the European Research Council under an Advanced Fellow Grant. The review of this paper was coordinated by Prof. H.-F. Lu.

P. Yang is with the National Key Laboratory of Science and Technology on Communications, University of Electronic Science and Technology of China, Chengdu 611731, China, and also with the School of Electronics and Computer Science, University of Southampton, Southampton SO17 1BJ, U.K. (e-mail: yangping19831117@yahoo.cn).

Y. Xiao and S. Li are with the National Key Laboratory of Science and Technology on Communications, University of Electronic Science and Technology of China, Chengdu 611731, China (e-mail: xiaoyue@uestc.edu.cn; lsq@uestc.edu.cn).

L. Hanzo is with the School of Electronics and Computer Science, University of Southampton, Southampton SO17 1BJ, U.K. (e-mail: lh@ecs.soton.ac.uk).

Color versions of one or more of the figures in this paper are available online at <http://ieeexplore.ieee.org>.

Digital Object Identifier 10.1109/TVT.2013.2274482